Pergamon

Geochimica et Cosmochimica Acta, Vol. 63, No. 19/20, pp. 3183–3191, 1999

0016-7037/99 $20.00 + .00

PII S0016-7037(99)00225-2

Silicates

Acidic dissolution of plagioclase: In-situ observations by hydrothermal atomic force microscopy

GUNTRAM JORDAN,[1,*] STEVEN R. HIGGINS,[1] CARRICK M. EGGLESTON,[1] SUSAN M. SWAPP,[1] DAWN E. JANNEY,[2] and KEVIN G. KNAUSS[3]

[1] Department of Geology and Geophysics, University of Wyoming, Laramie, WY 82071-3006, USA
[2] Departments of Geology and Chemistry/Biochemistry, Arizona State University, Tempe, AZ 85287-1404, USA
[3] Earth Science Division, Lawrence Livermore National Laboratory, Livermore, CA 94550, USA

(*Received October* 15, 1998; *accepted in revised form April* 29, 1999)

Abstract—Hydrothermal atomic force microscopy (HAFM) provides in situ access to the surfaces of dissolving crystals at temperatures above the ambient boiling point of water. Here, we applied HAFM to the (001) surfaces of labradorite and anorthite at temperatures up to 125°C. In HCl solutions (pH 2) we observed the formation of a rough and soft surface layer on both minerals. By applying high loading forces to the scanning tip, the soft layer can be removed and the underlying interface (between the fresh solid and the altered layer) can be observed. In this way, in situ information about the thickness of the altered layer on plagioclase and the morphology of the underlying interface can be obtained. On labradorite, the thickness of this layer does not exceed about 30 nm within the first 5 hr of exposure to acidic solution at 125°C, but on anorthite thicknesses of up to about 300 nm were observed. The uncovered interface on anorthite shows a nonuniform morphology and either appears rough in AFM images or shows a step-like pattern.

On anorthite, etch pits spread underneath the altered layer. This suggests that material must be released and transported through the layer without obvious changes in morphology of the layer's surface. Based on the rate of spreading of etch pits, the dissolution rate was calculated to be about 2×10^{-6} mol m^{-2} s^{-1} at 125°C. This value agrees reasonably well with literature data and supports the suggestion that dissolution mainly takes place underneath the altered layer and not on its surface. *Copyright © 1999 Elsevier Science Ltd*

1. INTRODUCTION

Feldspars are the most abundant minerals in the Earth's crust. Because of this abundance and the overwhelmingly huge interfacial area between the Earth's crust and hydrosphere, the chemical composition of our environment is significantly influenced by reactions at the interfaces of feldspars with aqueous solutions (i.e., by weathering). Perhaps the most globally significant longterm consequence of plagioclase weathering is in atmospheric CO_2 drawdown (e.g., Berner, 1995). If we can understand the key mechanisms of plagioclase dissolution, we obtain an understanding of how a particular molecular-scale process can affect global climate.

During dissolution in acidic aqueous solution under defined laboratory conditions, feldspars generally develop an altered surface layer. The presence of this altered or leached layer on feldspars has been reported often in the literature (e.g., Casey et al., 1989; Chou and Wollast, 1984; Hellmann et al., 1990; Muir et al., 1990). However, evidence for the presence of an altered layer coming from ex situ (e.g., vacuum) methods raises questions about the relationship of the results to in situ conditions. For example, an amorphous layer was observed on labradorite by transmission electron microscopy (TEM), but scanning electron microscopy (SEM) images taken after exposure to acidic solution (pH = 1) showed that the outermost layer spalls from the crystals (Casey et al., 1989). In addition, X-ray photoelectron spectroscopy (XPS) data obtained after acidic dissolution, or non-stoichiometric release rates during dissolution, could be affected by preferential dissolution at exsolution lamellae (Inskeep et al., 1991). By means of the newly designed hydrothermal atomic force microscope (Higgins et al., 1998a) it is now possible to directly observe the solid-liquid interface at a resolution high enough for imaging the formation and subsequent behavior of an altered layer.

The focus of this study is to evaluate and quantify the effect of an altered layer on the dissolution of plagioclase, and, if possible, to gain information about possible dissolution mechanisms related to this altered layer. In parallel, conventional TEM studies were carried out in an attempt to identify crystallographic features that might influence dissolution behavior. For our study, we chose albite (Higgins et al., 1998b), labradorite (An_{60}), and anorthite (An_{96}) in order to investigate a range of possible plagioclase dissolution behaviors. For example, for anorthite in acidic solution, stoichiometric release rates and dissolution rates independent of the Al solution concentration have been reported (Amrhein and Suarez, 1992; Oelkers and Schott, 1995). Furthermore, assuming a perfectly ordered structure in anorthite (An_{96}), bridging Si-O-Si (siloxane) linkages are nearly absent, so formation of an Si-rich, altered layer by leaching seems improbable (e.g., Blum and Stillings, 1995).

*Address reprint requests to Guntram Jordan, Institut für Mineralogie, Ruhr-Universität Bochum, Universitätsstr. 150, 44780 Bochum, Germany (Guntram.Jordan@ruhr_uni_bochum.de).

In contrast, relatively thick leached or altered layers are known to form on albite and labradorite (e.g., see refs. above).

2. EXPERIMENTAL DETAILS

The experiments presented here were conducted using a hydrothermal atomic force microscope (HAFM) operating in contact mode. The HAFM, designed in our laboratories, enables in situ AFM imaging of the solid-liquid interface at temperatures above the ambient boiling point of water by pressurizing both the fluid cell and the scanner housing. The pressure applied was 6.8 bar N_2. Details of the HAFM are described in Higgins et al. (1998a). We used contact-Si-cantilevers with integrated tips (Nanosensors, Germany; spring constant: ~0.2 N/m). The acidic solutions were prepared by adding reagent grade HCl to deionized water (resistivity: 18 MΩ cm). The solution was adjusted to pH 2 at room temperature. Flow rate through the fluid cell was typically 6 μL/s. Varying the flow between 3 and 12 μL/s gave no significant change in experimental results.

The anorthite crystals were from Miyakesima, Japan, and the labradorite crystals were from Chihuahua, Mexico. The chemical composition of both feldspars was examined using an electron microprobe. The average compositions of the anorthite and labradorite were $Ca_{0.96}Na_{0.04}Al_{1.93}Si_{2.05}O_8$ and $Ca_{0.58}Na_{0.39}K_{0.02}Al_{1.57}Si_{2.41}O_8$, respectively. Unit cell parameters for both anorthite and labradorite are $a \cong 8.2$ Å, $b \cong 12.9$ Å, $c \cong 14.2$ Å, $\alpha \cong 93°$, $\beta \cong 116°$, $\gamma \cong 91°$ (Wenk and Kroll, 1984; Müller et al., 1972). The crystals were cleaved with a knife edge parallel to (001) immediately prior to mounting in the HAFM under a passivated Ti wire (without any adhesives). The entire (geometric) surface area of the crystal exposed to solution typically was about 10 mm^2. The volume of the fluid cell is about 600 mm^3.

For TEM analysis, anorthite samples were prepared by crushing a small grain in propanol, depositing a droplet of the resulting liquid on a holey carbon film on a standard copper mesh TEM grid, and air drying. TEM analyses used a JEOL 4000EX high-resolution transmission electron microscope operating at 400 kV. A small objective aperture was used in order to increase the contrast from small changes in lattice orientation.

3. RESULTS AND DISCUSSION

Feldspars present difficulties that other materials, such as calcite and barite, do not impose on AFM imaging and the interpretation of topographic features. The discontinuities in surface elevation that we can safely call "steps" on calcite, for example, may have a variety of possible interpretations on feldspars. In addition to steps, there are possibilities including discontinuities at boundaries between areas with different space groups, dislocations, twin planes, exsolution boundaries, antiphase boundaries, and other features that may have some topographic expression at the surface and which indicate changes in structure or composition that extend into the bulk material. In contrast, a true step is strictly a surface structure that simply indicates the edge of a new molecular layer of material on the surface. We cannot easily tell the difference between these features with HAFM. Therefore, when we use the term "steps" below, we refer to the topographic feature and not to any strict definition that excludes these other possible origins of step-like features on feldspar surfaces. Furthermore, we define the surface as the outer surface of the altered layer on feldspars (i.e., the altered layer–solution interface) and the "interface" as (presumably) the feldspar–altered layer interface.

On albite, we observed very little surface alteration (although the surface clearly roughened significantly during acid exposure). This reflects the fact that plagioclase dissolution rates decrease with decreasing An component together with the fact that the maximum temperature of the microscope (about 150°C) is apparently still too low to sufficiently accelerate albite dissolution for AFM observation. Thus, in the following we only present and discuss data for labradorite and anorthite.

3.1. Labradorite

Within the first 60 min of contact with acidic solution (pH 2, HCl) at room temperature, we could not detect any changes in surface morphology, indicating that the (001) surface of labradorite did not undergo dissolution or leaching to an extent observable by AFM. However, as the temperature reached 125°C in the fluid cell of the HAFM, the surface slowly roughened. Figures 1a–c show the roughening of the surface within the first 200 min at 125°C. Surface roughening subdues the topography of the small steps at terraces induced by cleaving the crystal. After initial roughening, large cleavage steps can still be observed throughout the whole period of the experiments (up to 5 hr at 125°C). The dissolution behavior at these large cleavage steps is not uniform. We found steps maintaining their pristine morphology without any obvious retreat, while others became roughened. Along these roughened steps, lines of small, irregularly shaped pits developed. Figure 1d shows the roughened cleavage steps with small pits after 100 min at 125°C. These pits are very similar to the pits observed using AFM by Lee et al. (1998) at dislocations along the edges of albite exsolution lamellae in microperthite.

Along with roughening, the surface becomes soft. Loading forces of <10 nN do not cause observable surface damage, but application of higher loading forces with the AFM tip leads to removal of the soft surface layer and reveals an interface underneath with a hardness comparable to the hardness of the original labradorite surfaces in air. The depth of the scan fields produced by scanning with high loading force and then imaging a larger area at lower loading force can be used to estimate the thickness of the soft layer. Because the removal of the soft surface layer by the scanning tip mainly results from horizontal (frictional) forces, differences in tip shapes or apex radii of tips should not affect the depth of the scanfield, although we cannot completely rule out minor artifactual influences such as compression rather than removal. Despite this uncertainty, acquisition of in situ data on the thickness of the soft surface layer by HAFM remains valuable because they offer a means of comparison with ex situ measurements or calculations of the thickness of the altered layer based on non-stoichiometric elemental release rates. A "surface average" altered layer thickness calculated from release stoichiometry may be significantly different than local altered layer thickness if, for example, preferential dissolution or leaching at different exsolution lamellae (Inskeep et al., 1991) sufficiently skew the stoichiometric results. Moreover, altered layer thicknesses from XPS or other vacuum techniques may be skewed by in-vacuum condensation, or spalling of altered material (Casey et al., 1989).

On labradorite, we found that the thickness of the soft altered layer did not exceed 29 ± 19 nm in the first 5 hr at 125°C. The uncovered interface within scan fields shows the same morphology as the surface (Fig. 1e, f), suggesting that on labradorite the morphology of the surface of the altered layer and of the underlying interface changed simultaneously during the period the crystals were exposed to the solution. It should be remembered, however, that these images only show initial

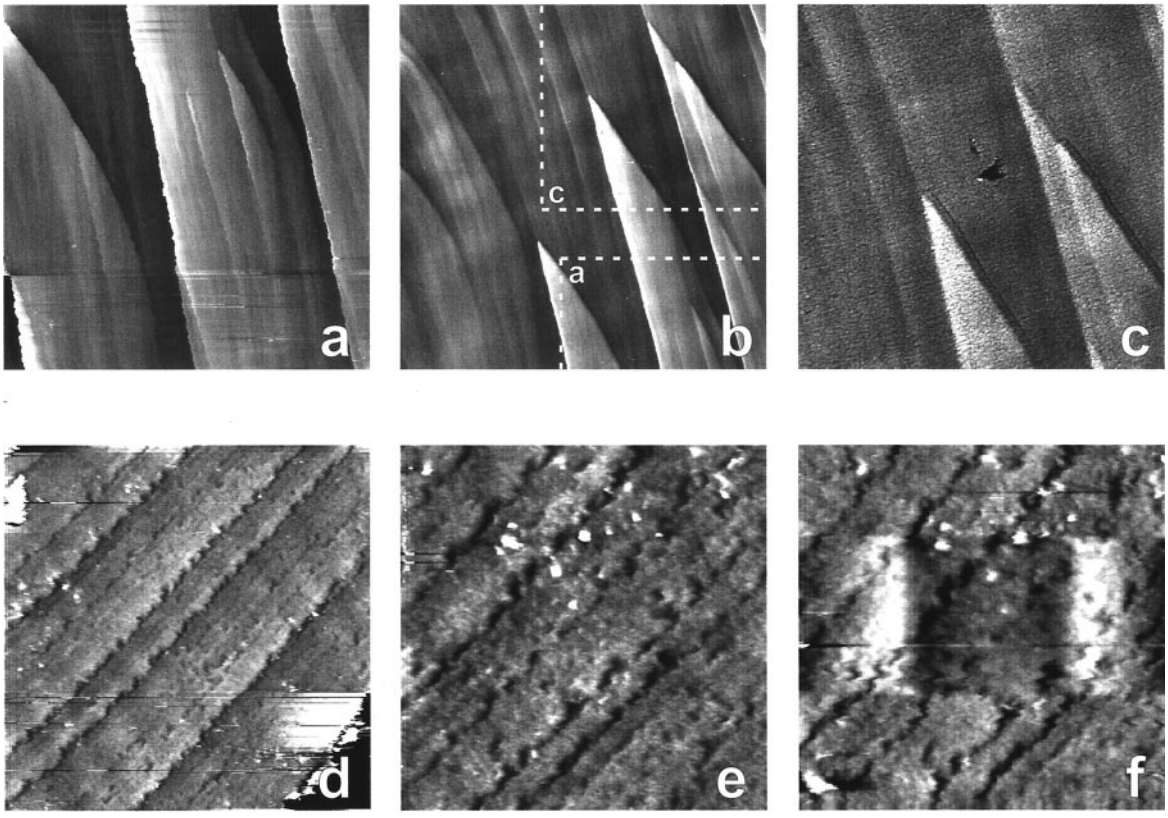

Fig. 1. (a–c) Sequence of images labradorite at 125°C showing roughening of the surface. (a) After 15 min exposure to acidic solution, the cleavage morphology still prevails on the surface (image size: 21 × 21 μm^2). (b) 47 min later the surface slowly becomes rough (image size: 30 × 30 μm^2). (c) 133 min later a rough and soft layer has formed but high cleavage steps are still discernable. The behavior of the cleavage steps is not uniform—here, the steps remain straight (compare to d–f). Step retreat is not obvious. (image size: 20 × 20 μm^2; note: the hole in the image center is caused artificially by high loading forces). (d–f) Sequence of images of labradorite at 125°C showing the formation of rough steps and the removal of the soft surface layer. (d) At 98 min exposure to acidic solution not only the surface but also the cleavage steps become rough (image size: 17 × 17 μm^2). (e) At the steps, lines of small pits develop (7 min later; image size: 9 × 9 μm^2). (f) Removal of the rough and soft surface layer by the scanning tip leaves a scan field (here: 15 ± 2 nm deep). The morphology of the surface within the scan field corresponds to the morphology of the surface before removing the layer (13 min later; image size: 9 × 9 μm^2; note: the ridges to the left and right of the scan field are artifacts caused by processing the image in order to show the morphology within the scan field).

dissolution of a fresh labradorite surface. An estimate of the volume of material released by dissolution can be made by assuming a dissolution rate between 10^{-7} and 10^{-9} mol m^{-2} s^{-1} in acidic solution at 125°C (rates and activation energies vary in the literature; for a review see Blum and Stillings, 1995). We estimate that a vertical retreat of the surface by 0.7 to 70 nm could be expected within 2 hr (calculated on the basis of mineral specific gravity of 2.7 g/cm^3). In comparison, we measure scan field depths of about 20 nm in this time.

3.2. Anorthite

In contrast to labradorite, freshly cleaved anorthite surfaces roughen very quickly in contact with acidic solution (pH 2, HCl). This surface roughening starts at room temperature, but is slow enough that it does not subdue the cleavage morphology of the surface completely. Large cleavage steps can still be observed in the AFM images. At room temperature, retreat of these cleavage steps was not observed within a period of about 30 min.

Heating to 75–90°C typically takes about 20–25 min. Because of rapid thermal drift during an increase in temperature, images cannot be obtained until microscope temperature stabilizes. Once drift has settled, the surface appears completely rough in the HAFM-images; even large cleavage steps can no longer be observed. The Root Mean Square (RMS) roughness of the surface is about 11 nm. The maximum relief (vertical distance between high point and low point) is about 30 nm. As with labradorite, the surface not only becomes rough, but also soft and the soft layer can be removed by the scanning tip. Figure 2 shows the depths of freshly created scan fields as a function of time on the anorthite (001) surface at 125°C. In the early stage of this experiment the thickness of the soft layer increased quickly, but after 2 hr at 125°C the thickness decreased again, to range between 50 and 100 nm. In other experiments (not shown), the thickness ranged between 150 and 300 nm. After the initial roughening and formation of the altered layer, no clear thickness increase with time could be found within the scatter in the data. We cannot exclude the

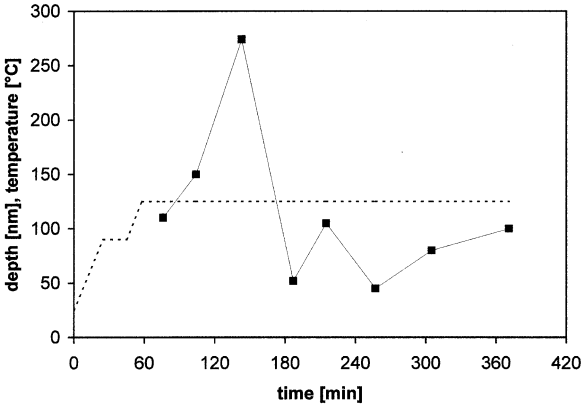

Fig. 2. The depth of freshly created scan fields vs. time (solid line) showing the thickness of the soft surface layer on anorthite in acidic solution at 125°C. All scan fields were created in close proximity. The dashed line in the diagram shows the temperature of the solution in the fluid cell during the experiment.

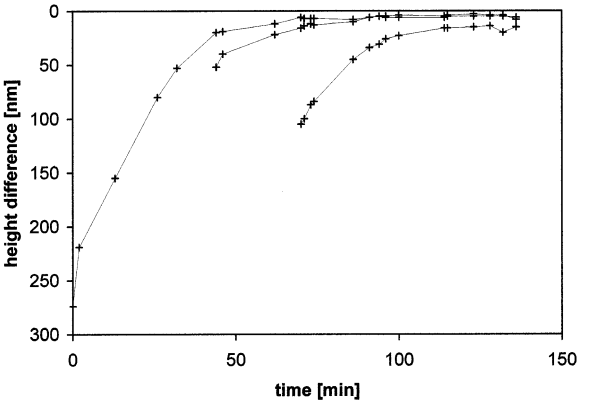

Fig. 4. Plot of the difference in height between the surface of the recurring altered layer within three scan fields and of the surrounding surface of the unaffected altered layer vs. time. Data were taken on anorthite at 125°C and show that scan fields heal (i.e., fill up with altered layer).

possibility that structural and compositional heterogeneities in the anorthite could lead to locally variable altered layer thickness and thus to the data scatter. Nevertheless, this altered layer is a ubiquitous presence on all three of the feldspars we have observed with HAFM. We conclude that this soft layer can be equated with a leached or otherwise altered layer resulting from exposure to acidic solution.

To investigate the formation of the soft layer at high temperatures, we removed it with the scanning tip, uncovering the interface within a scan field. On this uncovered interface, a new soft layer formed again immediately. In Fig. 3, three scan fields were created sequentially, with decreasing lateral size, at the same position. The depth of each successive (smaller) scan field shows the thickness of the newly formed soft layer in each former (larger) scan field. At first glance, one might assume that the reappearance of the altered layer in the scan fields could happen by accumulation (and repolymerization) of dissolved anorthite material on the entire surface, or by retreat of the entire interface with simultaneous conversion of anorthite into material building up the altered layer. In both possibilities, the apparent depths of scan fields (i.e., the difference in height between the surface of the recurred layer within a scan field and of the surrounding surface of the unmodified altered layer) should remain constant with time, and only the absolute thickness of the altered layer should increase with time. Our results, however, show neither an increase of the absolute layer thickness with time (Fig. 2) nor a constant apparent depth of scan fields. Figure 4 shows the difference in height between the surface of the re-formed layer in three subsequent scan fields and the surrounding surface. The height differences decrease with time; that is, the scan fields "heal" with time. Therefore, the altered layer must be formed within created scan fields preferentially, either by preferential accumulation of dissolved anorthite material on the scan field area or by enhanced retreat of the interface in the scan field area along with a conversion of anorthite into the material building up the altered layer (with an increase in volume). The latter should cause a lower interface within a healed scan field than in the surrounding area, and this lower interface should be detectable by creating a new, larger scan field after some reaction time. Although we attempted this experiment, the high loading forces required to image the interface, together with remnants of the soft layer under the scanning tip, caused poor image quality and we could not definitively detect such fields in the interface within the new, larger scan fields.

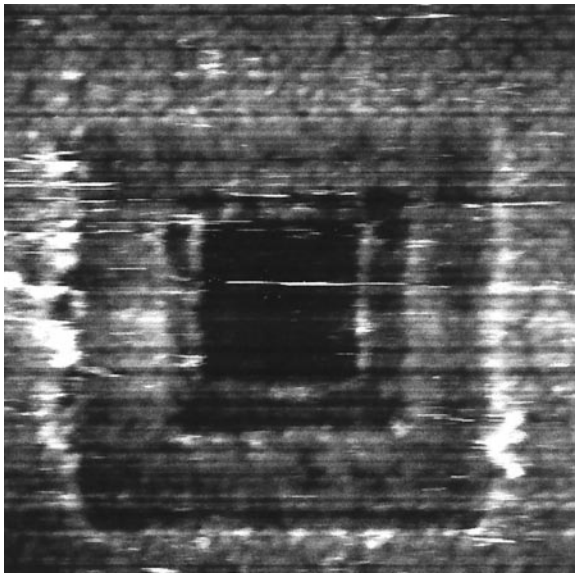

Fig. 3. The image shows three subsequently created scan fields with decreasing size on anorthite at 125°C (image size: $15 \times 15\ \mu m^2$). With respect to the uncovered interface in the smallest scan field, the thickness of the altered layer outside the scan fields is about 110 nm, in the outermost (first) scan field about 80 nm, and in the second about 50 nm. The first and second scan fields were created 17 and 10 min, respectively, before the image was taken. The third scan field was created immediately before this image was taken.

In contrast to labradorite, on which surface and interface morphology are the same (Fig. 1e, f), on anorthite the morphologies of uncovered interfaces could be divided into two groups (keeping in mind, however, that high loading forces

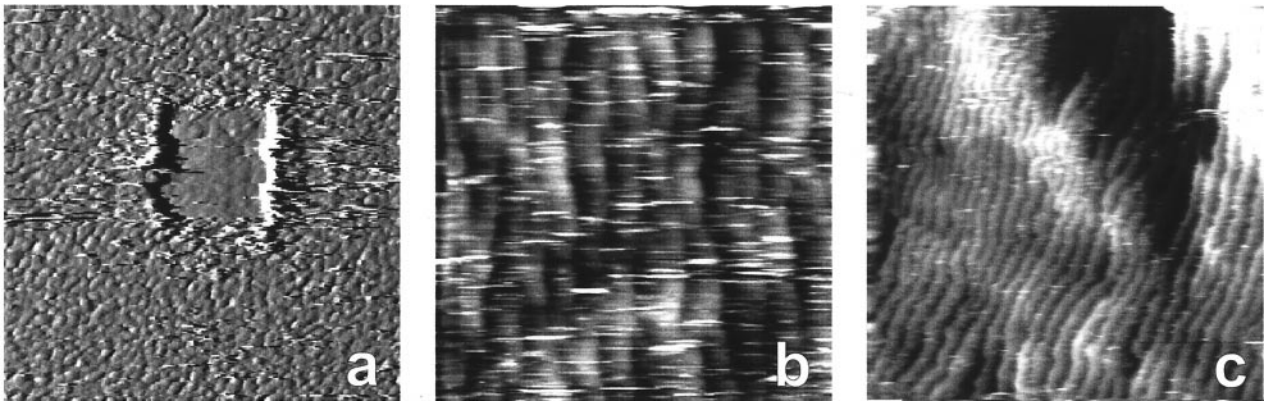

Fig. 5. The images show the variety of the morphology of the uncovered interface within scan fields on anorthite at 125°C. (a) The interface appears as rough as the surrounding surface (image size: 15 × 15 μm; slopes inclined to the left are bright). (b–c) The interface comprised of almost horizontal surface areas (maximum slope: (b) about 4°, (c) about 14°) with step-like features (image size: (b) 4 × 4 μm^2, (c) 10 × 10 μm^2).

were used to reveal the interface, so the interface is imaged at higher loading forces than the surface). In one group, the interface appears almost as rough as the surface itself (Fig. 5a), and in the other group the uncovered interface consists of step-like features (Fig. 5b, c). Although it is tempting to argue that this interface morphology shows steps and terraces according to the theories of Stranski (1928) and Burton et al. (1951), such micromorphology could also be a consequence of planar crystallographic features such as boundaries between regions with different space groups, twin planes, or exsolution lamellae.

Judging by the limiting compositions in which Huttenlocher exsolution has been observed ($An_{\sim 67}$ to $An_{\sim 90}$, Smith and Brown, 1988; Carpenter, 1994) and the composition of the anorthite (An_{96}; see above), exsolution seems to be an unlikely cause for stepped morphology as observed at the interface by HAFM. TEM attempts to identify microstructures that might cause steps on the surface were unsuccessful, perhaps because of the difficulty of recognizing them amidst the extensive brittle deformation introduced by crushing the sample. Individual dislocations and subgrain boundaries were not observed, suggesting a low dislocation density. Several instances of narrow twins were identified. Selected area electron diffraction patterns show the diffraction characteristics of a "transitional" anorthite (using the nomenclature of Gay, 1962): sharp *a* and *b* reflections, strongly streaked *c* reflections, and faint, strongly streaked *d* reflections. The *a* reflections are common to all plagioclases; *b* reflections are characteristic of the "body-centered anorthite" ($I\bar{1}$) structure, in which the number of Al-O-Al bonds is minimized by doubling the unit cell relative to albite and reversing the positions of Al and Si in the two halves (e.g., Wenk and Kroll, 1984); and *c* and *d* reflections result from a largely displacive phase transition characterized by slight shifts in atomic positions and corresponding distortion of the $I\bar{1}$ unit cell to produce the "primitive anorthite" ($P\bar{1}$) structure (e.g., Wenk and Kroll, 1984). The streaking of the *c* reflections is a consequence of intergrown domains with $I\bar{1}$ and $P\bar{1}$ structures on a scale of a few nm (McLaren, 1973). The Miyake anorthites are rapidly quenched high temperature plagioclases that occur together with volcanic glass (Müller et al., 1972) and thus probably have some residual disorder.

At the interface imaged within freshly created scan fields by HAFM, we found that the step-like features slowly retreat. Because of the difficulty of differentiating true motion of surface features from systematic drift, and because we were concerned that apparent motion could possibly be caused by preferential dissolution under the high tip loading forces needed to keep the interface free from restoration of a soft (altered) layer, we imaged large areas containing previously created scan fields (which served as fixed landmarks) in order to confirm that the step-like features indeed retreat across the interface underneath the soft layer. Figure 6 shows a pit edge approaching a scan field created on a flat surface. As the pit wall coincides with the scan field, the surface morphology at the edges of the scan field remains unaffected. Even as the etch pit moves under the scan field, the edges of the scan field are retained. Thus, without changing morphology at the edges, the scan field changes its vertical position. In other words, the whole scan field simply moves down the etch pit wall. This shows clearly that at least the majority of the loss of material from dissolution at etch pits does not occur at the surface but at deeper regions. In addition, on the surface within the scan field, movement of step-like features is observed. As observed for the edges of the scan fields, the morphology of the rough surface of the restored altered layer within the scan field appears to be unaffected by this step-like movement—only the vertical position of these features changes (like moving an object beneath a blanket). Since the scan field was created 10 min before the pit coincided with it, the soft layer within the scan field is still thin and presumably not capable of screening the step-like movement to the extent that the thicker soft layer beside the field does (i.e., the difference is like covering a staircase beneath a thin versus a thick blanket). Removal of material by dissolution, therefore, must be occurring even beneath the surface of the restored altered layer within the scan field. The most likely place for the removal of material by step-like movement is the interface.

The removal of a considerable amount of material from beneath the soft surface layer during dissolution is a viable mechanism only if material is transferred through the soft layer either completely or partially (if the other part of material serves to form the soft layer). However, we cannot say defin-

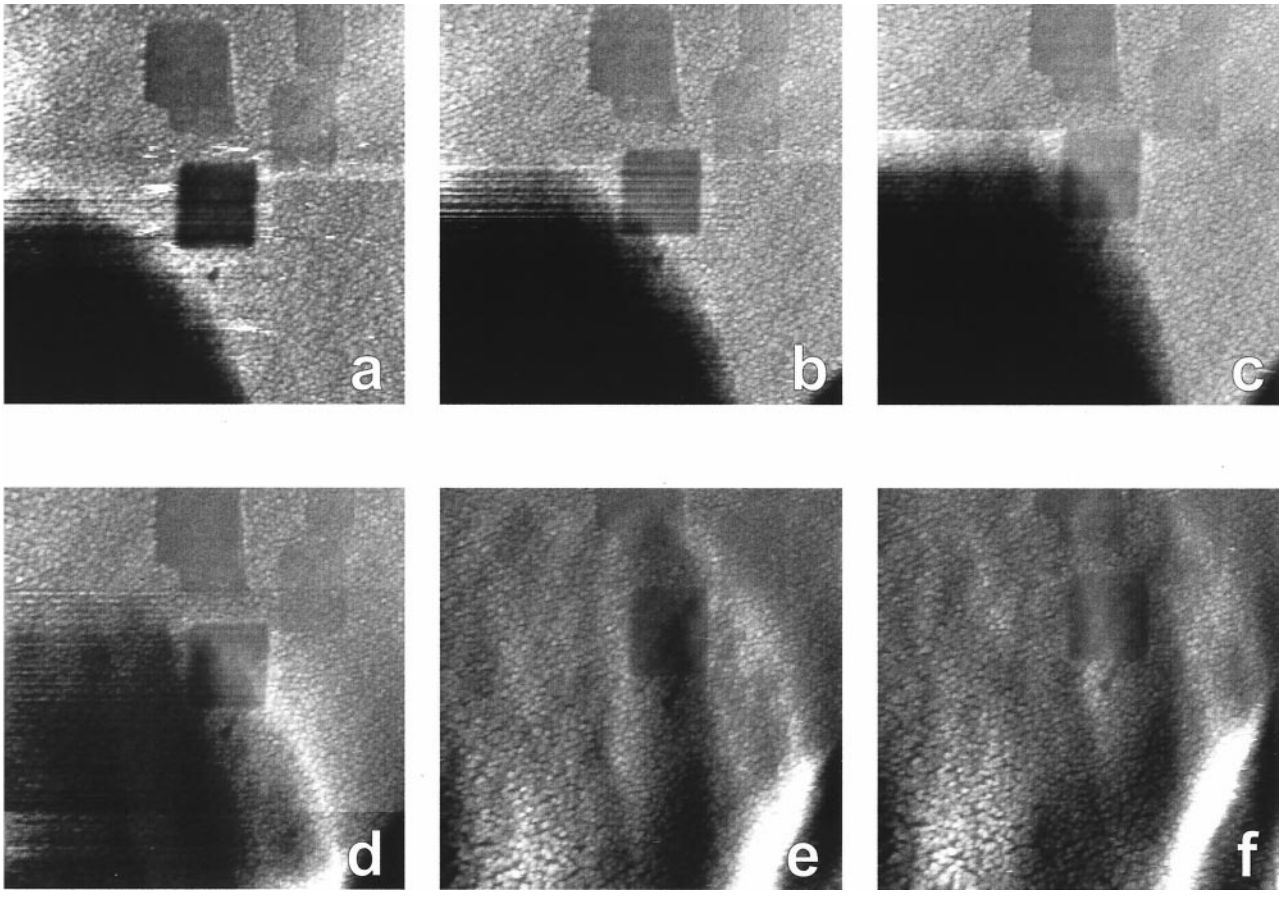

Fig. 6. Sequence of images showing anorthite dissolution at 125°C (image size: 20 × 20 μm^2). (a) An etch pit in the lower left of the image is growing towards a scan field in the center of the image. (b) 8 min later as the etch pit intersects with the scan field, the morphology of the scan field edges remain unaffected. (c–d) Underneath the still thin altered layer within the scan field (although hard to see), step-like movement can be observed ((c) 5 min later, (d) 4 min later). (e) 12 min later the edge of the pit wall has passed the scan field. (f) 9 min later, a new pit approaches from the lower right. Note: in image (e) and (f) the etch pit is still present but the images are processed in such a way that the area within the etch pit wall becomes visible.

itively, on the basis of our data, whether mass transport through the altered layer is a rate-controlling process. If it is rate-controlling in dissolution, we might expect in a future study, to observe interstep interaction by overlapping diffusion fields (such as by surface diffusion or by diffusion through a boundary layer) within the altered layer.

In general, the shape of etch pits on anorthite ranges between point bottomed triangular and ovoid. Similar etch pits were shown by Lundström (1970) on andesine and oligoclase. The etch pits grow by deepening vertically and spreading horizontally from their point of origin. Within the time frame of our experiments, the pits reach dimensions of up to several tens of μm and can easily be observed by SEM and optical microscopy. Figure 7 shows an SEM image of the anorthite surface after exposure to acidic solution for 4 hr (3 hr at 125°C). Within the etch pits, step-like features can clearly be observed.

A calculation of the anorthite dissolution rate can be made from our images by measuring the rate of expansion of etch pits. We define the "hinge point" as the intersection between the pit wall and the surrounding flat surface; the hinge point forms a closed loop around each pit that expands across the

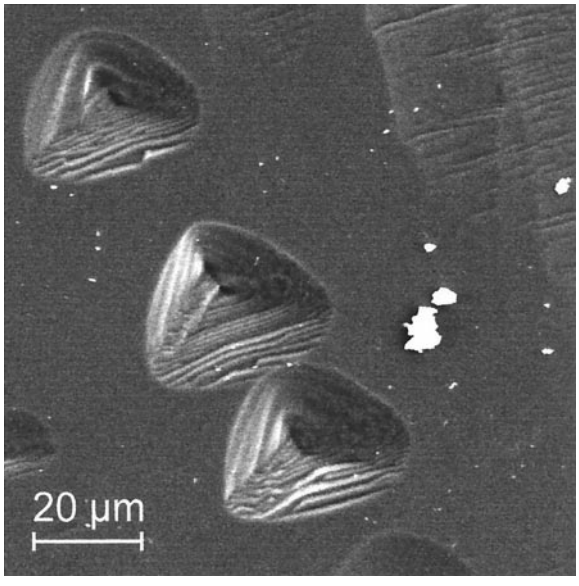

Fig. 7. SEM image of anorthite exposed to acidic solution for 4 hr (3 hr of that was at 125°C).

surface as the pit grows. By measuring the slopes of pit walls, and the rates of motion of the hinge point in different locations, we obtain a measure of how much faster the pit wall must be retreating compared with the flat surface in which the pit is forming. We then make several assumptions. First, we assume that the hinge points move exclusively laterally; i.e., that the flat surface in which the pit is forming maintains a zero retreat rate. There is some evidence for this; at 25°C and pH 3, very low or zero dissolution rates on pristine anorthite cleavage surfaces have been reported to persist even after 168 hr (Lasaga et al., 1998). Second, we assume that the thickness of the altered layer is constant. Third, we assume that the surface is at topographic steady state (defined below). Under these assumptions, we obtained a dissolution rate of 2×10^{-6} mol m^{-2} s^{-1} for anorthite (001) at 125°C (calculated using specific gravity = 2.75 g/cm^3).

Assumption 3 (that of topographic steady state) means that only removal of material at etch pit walls is considered. Our estimate thus applies only to a surface on which etch pits have coalesced to the point that no pristine surface remains between them. Overall dissolution can then be described either by the behavior of pit walls only, or a surface on which areas outside the etch pits have the same dissolution rate as within the pits as a result of unbound steps (e.g., Higgins et al., 1998c; Jordan and Rammensee, 1998). Considering the assumptions inherent to our calculation, our result agrees remarkably well with the data of Oelkers and Schott (1995) whose empirical rate law predicts a rate of 3.1×10^{-6} mol m^{-2} s^{-1} at 125°C and pH 2.

The Oelkers and Schott (1995) work is based on a normalization of rate to BET surface area, whereas our work is based on geometric surface area from AFM. It might appear at first glance that their rate law and our estimate are not strictly comparable. However, their reported BET specific surface area was, at most, a factor of 2 larger than the geometric specific surface area calculated for the particles used in their study. In addition, on a fresh cleavage surface, there is little difference between a geometric AFM surface area and a BET surface area. For example, fractal analysis of a series of 1 μm^2 image areas on a fresh anorthite (001) cleavage surface showed only a 4% increase in surface area if each individual pixel area was summed after taking microscopic roughness into account. Certainly, after initial roughening, a BET measurement would include increased surface area resulting from the new surface area in the altered layer. Our rate estimate, however, allows us to ignore the new surface area in the altered layer. Because of the small difference between the AFM geometric area and a BET area, our rate estimate is comparable to rates normalized to initial BET surface area. Our dissolution rate estimate, together with topographic HAFM observations, suggest that at steady state the majority of material release measured in macroscopic wet-chemical dissolution rate experiments can be attributed to dissolution at the interface by retreat of etch-pit walls, and not at the surface of the altered layer (whose morphology appears to be unaffected as the pit walls retreat beneath).

We examined our samples by AFM in air after the experiments (ex situ). The resulting images show that the anorthite surface changes while drying. Figure 8 shows an etch pit on anorthite, imaged in air after being exposed to acidic solution for 9 hr (at 125°C for 6 hr). The surface can be divided into 2 parts: 1. a rough part covering the step-like pit wall on the left side of the image and terminating in the shallower central part of the pit; and 2. a smoother part on the right side of the image where the pit consists partially of step-like patterns. The surface of the left part of the image is considerably harder than the soft, altered layer we encountered in our in situ observations. The height of the step between the left and the right part of the surface is 38 ± 16 nm. These observations suggest that the soft layer detected in situ has changed its physical properties while drying. We speculate that the layer, once moved from solution into air, contracts with dehydration and repolymerization of residual material and thus only partially covers the anorthite. This is consistent with the observations of Casey et al. (1989), who showed that an altered surface layer spalls off surfaces of labradorite in SEM images taken after the crystal had been reacted for 264 hr at pH 1 and 45°C.

Fig. 8. Anorthite in air after exposure to acidic solution for 9 hr (at 125°C for 6 hr; image size: 15.6 × 15.6 μm; slopes inclined to the left are bright). An etch pit can be seen. The walls of the pit show a step-like pattern. In the left part of the image, the surface is covered by a rough layer. The thickness of the layer measured at the step (labeled by arrows) to the surface in the right part of the image is 38 ± 16 nm.

At low pH, dissolution of sodic plagioclases involves exchange of Na^+ and Al^{3+} for protons followed by a slower breakdown of the (repolymerized) silica framework (e.g., Brantley and Stillings, 1996; Casey et al., 1988; Hellmann et al., 1990). This exchange leaves a protonated and partially linked framework of tetrahedral Si (the so called leached layer). On labradorite, TEM studies suggested that this leached layer is an amorphous, gel-like layer (Casey et al., 1989). In contrast to the sodic plagioclases, anorthite has a ratio of tetrahedral Si to Al of about 1. Leaching of aluminum, therefore, should leave isolated silica tetrahedra rather than a linked residual Si-framework (assuming a well ordered structure with alternating Al-O-Si bridges). Because the dissolution rate of anorthite shows no dependence on the Al-concentration in solution of pH 3 (Amrhein and Suarez, 1992) and at pH 2.4–3.2 (Oelkers and Schott, 1995), aluminum and silica release rates would be expected to

be congruent. Therefore, formation of a leached layer of residual silica would seem to be unlikely on anorthite. However, the in situ HAFM studies presented here show the formation of a physically, and presumably chemically, altered layer on anorthite surfaces that is very similar to the layer detected on labradorite and albite. We note that in the experiments of Oelkers and Schott (1995), preferential release of Al was observed in the initial stages of experiments, and that their XPS data are consistent with an Al-depleted surface layer (keeping in mind that their XPS results might be much less dramatic than would be the case if, akin to Fig. 8 above, the layer no longer covers the anorthite surface when it is subjected to vacuum). In addition, their XPS data are consistent with a decreased O/Si ratio on the reacted surfaces, also consistent with repolymerization within a residual silica layer.

The possibility that the soft layer observed in the HAFM could be a precipitate (resulting from the steady-state fluid cell composition) can be addressed by comparison of our fluid cell flow conditions to the flow conditions of Oelkers and Schott (1995). In our HAFM fluid cell, the ratio of geometric surface area of mineral in the fluid cell (S) to volume flow rate (Q) is $S/Q = 0.3 \pm 0.1$ min/cm, where S is estimated to be 0.1 cm^2. This S/Q value is at least 100 times smaller than that used by Oelkers and Schott (1995) who reported slight supersaturation only with respect to quartz in a few of their experiments. Thus, product concentrations inside our HAFM fluid cell should be a factor of 100 more dilute than those of Oelkers and Schott (1995).

On anorthite, therefore, we speculate that the soft layer we observe in HAFM is formed by silica partially repolymerizing during the dissolution process (perhaps aided by imperfect Al-Si ordering) at the surface. The quite constant layer thickness after an initial increase, and the healing of created scan fields, may indicate that accumulation of the layer preferentially occurs on the uncovered interface. As has already been studied extensively, such an altered layer is a steady-state phenomenon indicating that a greatly increased effective silica surface area within the layer must arise before all release rates become stoichiometric at steady state. In comparison, because the dissolution rate of labradorite is roughly 2–3 orders of magnitude lower than that of anorthite, the 5 hr of labradorite dissolution presented here corresponds to only about 18 to 180 s of anorthite dissolution. Even if the activation energy for anorthite dissolution is considerably lower than that of labradorite (see e.g., Blum and Stillings, 1995) and if the dissolution rates of anorthite and labradorite differ only by one order of magnitude at 125°C, we must be seeing only the initial stages of altered layer formation on labradorite. In addition, the process of formation of an altered layer might be different because of the presence of bridging Si-O-Si bonds.

4. CONCLUSIONS

The hydrothermal AFM provides in situ access to the evolution of microtopography on the surfaces of dissolving plagioclase feldspars, including quantification of altered surface layer formation kinetics and thickness. Our results strongly suggest that an altered layer forms on anorthite despite the (nominal) lack of bridging Si-O-Si linkages, and that at least within the time frame of the experiments, the thickness of this layer does not increase continuously but rather shows steady state behavior (e.g. by healing scan fields). There is a distinct interface between the altered layer and the underlying anorthite, and the morphology of this interface often shows step-like patterns. These results are consistent with the idea that dissolution takes place at this interface and not at the surface, and show that etch pits spread underneath the altered layer. The dissolution rate of anorthite can be closely approximated using an etch pit birth and spread model.

Despite these findings, many questions remain or are raised about the processes occurring at the altered-layer/anorthite interface. Among these questions are:

1. What are the step-like features on these feldspar surfaces, and what is their relation to the defect (twin, exsolution, etc.) features of feldspars?
2. Is it possible to describe feldspar dissolution in terms of a step-kinematic model such as Burton-Cabrera-Frank (1951) and its offspring?
3. Whether or not (2) is possible, what is the role of the altered layer in the dissolution process?

It should be possible to probe some of these questions by raising the pressure (and therefore temperature) limits of the HAFM so that we can reliably investigate the dissolution of a wider range of plagioclases.

Acknowledgments—We wish to thank Rolf Hollerbach (Mineralogisches Museum der Universität zu Köln) for kindly providing excellent samples, Susan L. Brantley, Kathryn L. Nagy and an anonymous reviewer for helpful comments. Furthermore the authors wish to thank the U.S. Department of Energy, Office of Basic Energy Science (#KC040302 to KGK, #DE-FG03-96SF14623 to CME), the National Science Foundation (#EAR-9634143 to CME), and the German Academic Exchange Service (DAAD) to GJ for financial support of this work and of the development of HAFM. Also, DEJ acknowledges the National Science Foundation (#EAR 9706359 to Peter R. Buseck) and the Center for High Resolution Electron Microscopy at ASU.

REFERENCES

Amrhein C. and Suarez D. L. (1992) Some factors affecting the dissolution kinetics of anorthite at 25°C. *Geochim. Cosmochim. Acta* **56,** 1815–1826.

Berner R. A. (1995) Chemical weathering and its effect on atmospheric CO2 and climate. In *Chemical Weathering of Silicate Minerals* (ed. A. F. White and S. L. Brantley), *Rev. Mineral.* **31,** 565–582. MSA.

Blum A. E. and Stillings L. L. (1995) Feldspar dissolution kinetics. In *Chemical Weathering of Silicate Minerals* (eds. A. F. White and S. L. Brantley), *Rev. Mineral.* **31,** 291–351. MSA.

Brantley S. L. and Stillings L. (1996) Feldspar dissolution at 25°C and low pH. *Am. J. Sci.* **296,** 101–127.

Burton W. K., Cabrera N., and Frank F. C. (1951) The growth of crystals and the equilibrium structure of their surfaces. *Phil. Trans. Royal Soc.* **A243,** 299–358.

Carpenter M. A. (1994) Subsolidus phase relations of the plagioclase feldspar solid solution. In *Feldspars and their Reactions* (ed. I. Parsons), *NATO ASI Series* **C421,** 221–269. Kluwer.

Casey W. H., Westrich H. R., and Arnold G. W. (1988) Surface chemistry of labradorite feldspar reacted with aqueous solutions at pH = 2, 3, and 12. *Geochim. Cosmochim. Acta* **52,** 2795–2807.

Casey W. H., Westrich H. R., Massis T., Banfield J. F., and Arnold G. W. (1989) The surface of labradorite feldspar after acid hydrolysis. *Chem. Geol.* **78,** 205–218.

Chou L. and Wollast R. (1984) Study of the weathering of albite at room temperature and pressure with a fluidized bed reactor. *Geochim. Cosmochim. Acta* **48,** 2205–2217.

Gay P. (1962) Sub solidus relations in the plagioclase feldspars. *Norsk Geol. Tidssk.* **42,** 37–56.

Hellmann R., Eggleston C. M., Hochella M. F. Jr., and Crerar D. A. (1990) The formation of leached layers on albite surfaces during dissolution under hydrothermal conditions. *Geochim. Cosmochim. Acta* **54,** 1267–1281.

Higgins S. R., Eggleston C. M., Knauss K. G., and Boro C. O. (1998a) A hydrothermal atomic force microscope for imaging in aqueous solution up to 150°C. *Rev. Sci. Instrum.* **69,** 2994–2998.

Higgins S. R., Eggleston C. M., Jordan G., Knauss K. G., and Boro C. O. (1998b) In-situ observation of oxide and silicate mineral dissolution by hydrothermal scanning force microscopy: Initial results for hematite and albite. *Mineral. Mag.* **62A,** 618–619.

Higgins S. R., Jordan G., Eggleston C. M., and Knauss K. G. (1998c) Dissolution kinetics of the barium sulfate (001) surface by hydrothermal atomic force microscopy. *Langmuir* **14,** 4967–4971.

Inskeep W. P., Nater E. A., Bloom P. R., Vandervoort D. S., and Erich M. S. (1991) Characterization of laboratory weathered labradorite surfaces using X-ray photoelectron spectroscopy and transmission electron microscopy. *Geochim. Cosmochim. Acta* **55,** 787–800.

Jordan G. and Rammensee W. (1998) Dissolution rates of calcite (10$\bar{1}$4) obtained by scanning force microscopy: Microtopography-based dissolution kinetics on surfaces with anisotropic step velocities. *Geochim. Cosmochim. Acta* **62,** 941–947.

Lasaga A. C., Lüttge A., MacInnis I. N., and Bolton E. W. (1998) Phase shift interferometry, near-atomic scale data, and a new view on fluid-rock reactions. *Mineral. Mag.* **62A,** 854–855.

Lee M. R., Hodson M. E., and Parsons I. (1998) The role of intragranular microtextures and microstructures in chemical and mechanical weathering: Direct comparisons of experimentally and naturally weathered alkali feldspars. *Geochim. Cosmochim. Acta* **62,** 2771–2788.

Lundström I. (1970) Etch-pattern and albite twinning in two plagioclases. *Arkiv för Mineralogi och Geologi* **5,** 63–91.

McLaren A. C. (1973) The domain structure of a transitional anorthite: A study by direct-lattice resolution electron microscopy. *Contrib. Mineral. Petrol.* **41,** 47–52.

Muir I. J., Bancroft G. M., Shotyk W., Nesbitt H. W. (1990) A SIMS and XPS study of dissolving plagioclase. *Geochim. Cosmochim. Acta* **54,** 2247–2256.

Müller W. F., Wenk H.-R., and Thomas G. (1972) Structural variations in anorthites. *Contrib. Mineral. Petrol.* **34,** 304–314.

Oelkers E. H. and Schott J. (1995) Experimental study of anorthite dissolution and the relative mechanism of feldspar hydrolysis. *Geochim. Cosmochim. Acta* **59,** 5039–5053.

Smith J. V. and Brown W. L. (1988) *Feldspar minerals 1. Crystal structures, physical, chemical, and microtextural properties*. 2nd ed. Springer.

Stranski I. N. (1928) Zur Theorie des Kristallwachstums. *Z. phys. Chem.* **136,** 259–278.

Wenk H.-R. and Kroll H. (1984) Analysis of P$\bar{1}$, I$\bar{1}$, and C$\bar{1}$ plagioclase structures. *Bull. Min.* **107,** 467–487.